PRAMANA
— journal of
physics

Vol. 86, No. 2
February 2016
pp. 437–451

Neutrino mass bounds from neutrinoless double beta-decays and cosmological probes

YONG-YEON KEUM

Institute of Basic Science, Seoul National University, 1 Kwan-Ak-Ro, Kwan-Ak-Gu, Seoul, Republic of Korea
E-mail: yykeum2011@snu.ac.kr; yyk2008@hanmail.net

DOI: 10.1007/s12043-015-1164-8; ***e*Publication:** 21 January 2016

Abstract. We investigate the way the total mass sum of neutrinos can be constrained from the neutrinoless double beta-decay and cosmological probes with cosmic microwave background (CMBR), large-scale structures including 2dFGRS and SDSS datasets. First we discuss, in brief, the current status of neutrino mass bounds from neutrino beta decays and cosmic constraint within the flat ΛCMD model. In addition, we explore the interacting neutrino dark-energy model, where the evolution of neutrino masses is determined by quintessence scalar field, which is responsible for cosmic acceleration. Assuming the flatness of the Universe, the constraint we can derive from the current observation is $\sum m_\nu < 0.87$ eV at 95% confidence level, which is consistent with $\sum m_\nu < 0.68$ eV in the flat ΛCDM model without Lyman alpha forest data. In the presence of Lyman-α forest data, interacting dark-energy models prefer a weaker bound $\sum m_\nu < 0.43$ eV to $\sum m_\nu < 0.17$ eV (Seljark *et al*). Finally, we discuss the future prospect of the neutrino mass bound with weak-lensing effects.

Keywords. Neutrino masses; neutrinoless double beta decay; large-scale structures; interacting neutrino dark-energy model.

PACS Nos 13.15.+g; 14.60.Pq; 14.60.St; 95.36.+x; 95.75.−z

1. Neutrino mass bounds from neutrinoless double beta decays

The standard method for measuring absolute value of the neutrino mass is based on the detailed investigation of the high-energy part of the β-spectrum of the decay of tritium:

$$^3\mathrm{H} \longrightarrow {}^3\mathrm{He} + e^- + \bar{\nu}_e. \tag{1}$$

This decay has a small energy release ($E_0 \simeq 18.6$ keV) and a convenient lifetime ($T_{1/2} = 12.3$ yr). As the flavour eigenstates are different from mass eigenstates in neutrino sector, in general, electron neutrino can be expressed as

$$\nu_{eL} = \sum_i U_{ei}\, \nu_{iL}, \tag{2}$$

where ν_i is the field of neutrino with mass m_i and U is the unitary mixing matrix. Neglecting the recoil of the final nucleus, the spectrum of the electrons is given by

$$\frac{\mathrm{d}\Gamma}{\mathrm{d}E} = \sum_i |U_{ei}|^2 \frac{\mathrm{d}\Gamma_i}{\mathrm{d}E}, \tag{3}$$

and the resulting spectrum can be analysed in terms of a single mean-squared electron neutrino mass

$$\langle m_\beta \rangle^2 = \sum_j m_j^2 |U_{ej}|^2 = m_1^2 |U_{e1}|^2 + m_2^2 |U_{e2}|^2 + m_3^2 |U_{e3}|^2. \tag{4}$$

If the neutrino mass spectrum is practically degenerate, $m_1 \simeq m_2 \simeq m_3$, the neutrino mass can be measured in these experiments. Present-day tritium experiments Mainz [1] and Troitsk [2] gave the following results:

$$m_1^2 = (-1.2 \pm 2.2 \pm 2.1)\ \mathrm{eV}^2 \quad \text{(Mainz)}, \tag{5}$$

$$= (-2.3 \pm 2.5 \pm 2.0)\ \mathrm{eV}^2 \quad \text{(Troitsk)}. \tag{6}$$

This value corresponds to the upper bound

$$m_1 < 2.2\ \mathrm{eV} \quad (95\%\ \mathrm{CL}). \tag{7}$$

Another useful method is by using the neutrinoless double beta ($0\nu\beta\beta$) decay. The search for neutrinoless double β-decay

$$(A, Z) \longrightarrow (A, Z_2) + e^- + e^- \tag{8}$$

for some even–even nuclei is the most sensitive and direct way of investigating the nature of neutrinos with definite masses. In this process, total lepton number is violated ($\Delta L = 2$) and is allowed only if massive neutrinos are Majorana particles. The rate of $0\nu\beta\beta$-decay is approximately

$$\frac{1}{T_{1/2}^{0\nu}} = G_{0\nu}(Q_{\beta\beta}, Z) |M_{0\nu}|^2 \langle m_{\beta\beta} \rangle^2, \tag{9}$$

where $G^{0\nu}$ is the phase-space factor for the emission of the two electrons, $M_{0\nu}$ is the nuclear matrix element and $\langle m_{\beta\beta} \rangle$ is the effective Majorana mass of the electron neutrino:

$$\langle m_{\beta\beta} \rangle \equiv \left| \sum_i U_{ei}^2 m_i \right|. \tag{10}$$

We can write eq. (10), for normal and inverted hierarchy respectively, in terms of mixing angles and $\Delta_s^2 = m_2^2 - m_1^2 = (7.9^{+2.8}_{-2.9}) \cdot 10^{-5}\ \mathrm{eV}^2$, $\Delta_a = \pm(m_3^2 - m_2^2) \simeq \pm(2.6 \pm 0.2) \cdot 10^{-3}\ \mathrm{eV}^2$ and CP phases as follows:

Normal hierarchy:

$$\langle m_{ee} \rangle = \left| c_2^2 c_3^2 m_1 + c_2^2 s_3^2 \mathrm{e}^{i\phi_2} \sqrt{\Delta_s^2 + m_1^2} + s_2^2 \mathrm{e}^{i\phi_3} \sqrt{\Delta_a^2 + m_1^2} \right|.$$

Inverted hierarchy:

$$\langle m_{ee} \rangle = \left| s_2^2 m_1 + c_2^2 s_3^2 \mathrm{e}^{i\phi_2} \sqrt{\Delta_a^2 - \Delta_s^2 + m_1^2} + c_2^2 s_2^2 \mathrm{e}^{i\phi_3} \right|. \tag{11}$$

From these relations, we can have the correlation plot between m_{light} and $|m_{\beta\beta}|$ with currently observed datasets of mixing angles and $\Delta^2_{s,a}$ from neutrino oscillation experiments. However, $0\nu\beta\beta$ decays have not yet been seen experimentally.

The most stringent lower bounds for the time of life of $0\nu\beta\beta$-decay were obtained in the Heidelberg–Moscow [4] and IGEX [5] ^{76}Ge experiments:

$$T^{0\nu}_{1/2} \geq 1.9 \cdot 10^{25} \text{ yr} \quad (90\% \text{ CL}) \quad \text{Heidelberg–Moscow}, \tag{12}$$

$$T^{0\nu}_{1/2} \geq 1.57 \cdot 10^{25} \text{ yr} \quad (90\% \text{ CL}) \quad \text{IGEX}. \tag{13}$$

Taking into account different calculations of the nuclear matrix elements, from these results, the following upper bounds were obtained for the effective Majorana mass:

$$|m_{\beta\beta}| \ < \ (0.35-1.24) \text{ eV}. \tag{14}$$

Many new experiments (including CAMEO, CUORE, COBRA, EXO, GENIUS, MAJORANA, MOON and XMASS experiments) on the search for neutrinoless double β-decay are in preparation at present. In these experiments, sensitivities

$$|m_{\beta\beta}| \simeq (0.1 - 0.015) \text{ eV} \tag{15}$$

are expected to be achieved. The detailed upper limit of $|m_{\beta\beta}|$ and the sensitivities of the future $0\nu\beta\beta$-decay experiments are summarized in table 1. It is very difficult to confirm the normal hierarchy pattern of neutrino mass when $m_1 < 1.7 \cdot 10^{-3}$ eV. However, for the inverted case, it can be detected if $m_3 < 8.9 \cdot 10^{-3}$ eV and $m_{ee} > 0.012$ eV.

Table 1. The current upper limits on the effective Majorana neutrino mass $|m_{\beta\beta}|$ and the sensitivities of the future $0\nu\beta\beta$-decay experiments. We used the matrix elements $M^{0\nu}$ with reduced uncertainty [3]. $T^{0\nu}_{1/2}$ denotes the current lower limit on the $0\nu\beta\beta$-decay half-life or the sensitivity of planned $0\nu\beta\beta$-decay experiments.

Nucleus	$M^{0\nu}$	$T^{0\nu}_{1/2}$ (yr)	Experiment	$\lvert m_{\beta\beta}\rvert$ (eV)
^{76}Ge	2.40	$1.9 \cdot 10^{25}$	Heidelberg–Moscow	0.55
		$3 \cdot 10^{27}$	Majorana	0.044
		$7 \cdot 10^{27}$	GEM	0.028
		$1 \cdot 10^{28}$	GENIUS	0.023
^{100}Mo	1.16	$6.0 \cdot 10^{22}$	NEM03	7.8
		$4 \cdot 10^{24}$	NEM03	0.92
		$1 \cdot 10^{27}$	MOON	0.058
^{130}Te	1.50	$1.4 \cdot 10^{23}$	CUORE	3.9
		$2 \cdot 10^{26}$	CUORE	0.10
^{136}Xe	0.98	$1.2 \cdot 10^{24}$	DAMA	2.3
		$3 \cdot 10^{26}$	XMASS	0.10
		$2 \cdot 10^{27}$	EXO(1t)	0.055
		$4 \cdot 10^{28}$	EXO(10t)	0.012

2. Neutrino mass bounds from cosmological constraints within the standard cosmology

Within the standard cosmological model, the relic abundance of neutrinos at the present epoch comes out straightforwardly from the fact that they follow the Fermi–Dirac distribution after freeze-out, and their temperature is related to the CMB radiation temperature $T_{\rm CMB}$ today by $T_\nu = (4/11)^{1/3} T_{\rm CMB}$ with $T_{\rm CMB} = 2.726$ K, providing

$$n_\nu = \frac{6\zeta(3)}{11\pi^2}\, T_{\rm CMB}^3, \tag{16}$$

where $\zeta(3) \simeq 1.202$, which gives $n_\nu \simeq 112\ {\rm cm}^{-3}$ for each family of neutrinos at present. By now the massive neutrinos become non-relativistic, and their contribution to the mass density (Ω_ν) of the Universe can be expressed as

$$\Omega_\nu h^2 = \frac{\Sigma}{93.14\ {\rm eV}}, \tag{17}$$

where Σ stands for the sum of the neutrino masses. In this relation, we include the effect of three neutrino oscillations [6]. We should notice that when obtaining the limit of neutrino masses one usually assumes

(a) the standard spatially flat ΛCDM model with adiabatic primordial perturbations,
(b) they have no non-standard interactions,
(c) neutrinos decoupled from the thermal background at the temperatures of order 1 MeV.

These simple conditions can be modified due to a sizable neutrino–antineutrino asymmetry, due to additional light scalar field coupled with neutrinos [7], and due to the light sterile neutrino [8]. However, analysis of WMAP and 2dFGRS data gave independent evidence for small lepton asymmetries [9,10], and such a scenario with a light scalar field is strongly disfavoured by the current CMB power spectrum data [11]. We shall not therefore take into account such non-standard couplings of neutrinos in the following. In addition, current cosmological observations are sensitive to neutrino masses $0.1\ {\rm eV} < \Sigma < 2.0\ {\rm eV}$. In this mass scale, the mass-square differences are small enough and all three active neutrinos are nearly degenerate in mass. Therefore, we assume degenerate mass hierarchy. Even if we consider a different mass hierarchy pattern, it will be very difficult to distinguish such hierarchy patterns from cosmological data alone [12].

After neutrinos decoupled from the thermal background, they stream freely and their density perturbations are damped on a scale smaller than their free-streaming scale. Consequently, the perturbations of cold dark matter (CDM) and baryons grow more slowly because of the missing gravitational contribution from neutrinos. The free-streaming scale of relativistic neutrinos grows with the Hubble horizon. When the neutrinos become non-relativistic, their free-streaming scale shrinks, and they fall back into the potential wells. The neutrino density perturbation with scales larger than the free-streaming scale resumes to trace those of the other species. Thus the free-streaming effect suppresses the power spectrum on scales smaller than the horizon when the neutrinos become non-relativistic. The co-moving wavenumber corresponding to this scale is given by

$$k_{nr} = 0.026 \left(\frac{m_\nu}{1\ {\rm eV}}\right)^{1/2} \Omega_m^{1/2}\, h\ {\rm Mpc}^{-1}, \tag{18}$$

for degenerated neutrinos, with almost the same mass m_ν. The growth of Fourier modes with $k > k_{nr}$ will be suppressed because of neutrino free-streaming. The power spectrum of matter fluctuations can be written as

$$P_m(k, z) = P_*(k)\, T^2(k, z), \tag{19}$$

where $P_*(k)$ is the primordial spectrum of matter fluctuations, to be a simple power law $P_*(k) = A\, k^n$, where A is the amplitude and n is the spectral index. Here the transfer function $T(k, z)$ represents the evolution of perturbation relative to the largest scale. If some fraction of the matter density (e.g., neutrinos or dark energy) is unable to cluster, the speed of growth of perturbation becomes slower. Because the contribution to the fraction of matter density from neutrinos is propotional to their masses (eq. (17)), the larger mass leads to the smaller growth of perturbation. The suppression of the power spectrum on small scales is roughly proportional to f_ν [21]:

$$\frac{\Delta P_m(k)}{P_m(k)} \simeq -8 f_\nu, \tag{20}$$

where $f_\nu = \Omega_\nu / \Omega_M$ is the fractional contribution of neutrinos to the total matter density. This result can be understood qualitatively from the fact that only a fraction $(1 - f_\nu)$ of the matter can cluster when massive neutrinos are present [22]. Analyses of CMB data are not sensitive to neutrino masses if neutrinos behave as massless particles at the epoch of last scattering. According to the analytic consideration in [23], as the redshift when neutrino becomes non-relativistic is given by $1 + z_{nr} = 6.24 \cdot 10^4\, \Omega_\nu\, h^2$ and $z_{\rm rec} = 1088$, neutrinos become non-relativistic before the last scattering when $\Omega_\nu h^2 > 0.017$ (i.e., $\Sigma > 1.6$ eV). Therefore, the dependence of the position and the height of the first peak on $\Omega_\nu h^2$ has a turning point at $\Omega_\nu h^2 \simeq 0.017$. This value also affects CMB anisotropy by modifying the integrated Sachs–Wolfe effect due to the massive neutrinos. However, the CMB data constrain other parameters that are degenerate with Σ. Also, as there is a range of scales common to the CMB and LSS experiments, CMB data provide an important constraint on the bias parameters. We summarize some of the recent cosmological neutrino mass bounds within the flat-ΛCDM model in table 2.

Table 2. Recent cosmological neutrino mass bounds (95% CL).

Cosmological dataset	Σ bound (2σ)	References
CMB (WMAP-3 year alone)	< 2.0 eV	Fukugita *et al* [13]
LSS[2dFGRS]	< 1.8 eV	Elgaroy *et al* [14]
CMB + LSS[2dFGRS]	< 1.2 eV	Sanchez *et al* [15]
”	< 1.0 eV	Hannestad [16]
CMB + LSS + SN1a	< 0.75 eV	Barger *et al* [17]
”	< 0.68 eV	Spergel *et al* [18]
CMB + LSS + SN1a + BAO	< 0.62 eV	Goobar *et al* [19]
”	< 0.58 eV	
CMB + LSS + SN1a + Ly-α	< 0.21 eV	Seljak *et al* [20]
CMB + LSS + SN1a + BAO + Ly-α	< 0.17 eV	Seljak *et al* [20]

3. Neutrino mass bounds in interacting neutrino-dark energy model

Using our previous works [24–26], we investigate the cosmological implication of an idea of the dark energy interacting with neutrinos [27,28]. For simplicity, we consider the case that dark energy and neutrinos are coupled such that the mass of the neutrinos is a function of the scalar field which drives the late-time accelerated expansion of the Universe.

In our scenario, equations for quintessence scalar field are given by

$$\ddot{\phi} + 2\mathcal{H}\dot{\phi} + a^2 \frac{\mathrm{d}V_{\mathrm{eff}}(\phi)}{\mathrm{d}\phi} = 0, \tag{21}$$

$$V_{\mathrm{eff}}(\phi) = V(\phi) + V_{\mathrm{I}}(\phi), \tag{22}$$

$$V_{\mathrm{I}}(\phi) = a^{-4} \int \frac{\mathrm{d}^3 q}{(2\pi)^3} \sqrt{q^2 + a^2 m_\nu^2(\phi)}\, f(q), \tag{23}$$

$$m_\nu(\phi) = \bar{m}_i \mathrm{e}^{\beta(\phi/M_{\mathrm{pl}})}, \tag{24}$$

where $V(\phi)$ is the potential of quintessence scalar field, $V_{nI}(\phi)$ is the additional potential due to the coupling to neutrino particles [28,29] and $m_\nu(\phi)$ is the mass of neutrino coupled to the scalar field, where we assume the exponential coupling with a coupling parameter β. $\mathcal{H}$ is $\dot{a}/a$, where the dot represents the derivative with respect to the conformal time τ.

Energy densities of mass-varying neutrino (MaVaNs) and quintessence scalar field are described as

$$\rho_\nu = a^{-4} \int \frac{\mathrm{d}^3 q}{(2\pi)^3} \sqrt{q^2 + a^2 m_\nu^2} f_0(q), \tag{25}$$

$$3P_\nu = a^{-4} \int \frac{\mathrm{d}^3 q}{(2\pi)^3} \frac{q^2}{\sqrt{q^2 + a^2 m_\nu^2}} f_0(q), \tag{26}$$

$$\rho_\phi = \frac{1}{2a^2}\dot{\phi}^2 + V(\phi), \tag{27}$$

$$P_\phi = \frac{1}{2a^2}\dot{\phi}^2 - V(\phi). \tag{28}$$

From eqs (25) and (26), the equation of motion for the background energy density of neutrinos is given by

$$\dot{\rho}_\nu + 3\mathcal{H}(\rho_\nu + P_\nu) = \frac{\partial \ln m_\nu}{\partial \phi}\dot{\phi}(\rho_\nu - 3P_\nu). \tag{29}$$

The evolution of neutrinos requires solving the Boltzmann equations in the case [24,25]:

$$\frac{\mathrm{d}q}{\mathrm{d}\tau} = -\frac{1}{2}\dot{h}_{ij} q n^i n^j - a^2 \frac{m}{q}\frac{\partial m}{\partial x^i}\frac{\mathrm{d}x^i}{\mathrm{d}\tau}. \tag{30}$$

Our analytic formula in eq. (30) is different from those of [30] and [31], because they have omitted the contribution of the varying neutrino mass term. The first-order Boltzmann equations written in the synchronous gauge reads [32] as

$$\frac{\partial \Psi}{\partial \tau} + i\frac{q}{\epsilon}(\hat{\mathbf{n}}\cdot\mathbf{k})\Psi + \left(\dot{\eta} - (\hat{\mathbf{k}}\cdot\hat{\mathbf{n}})^2 \frac{\dot{h} + 6\dot{\eta}}{2}\right)\frac{\partial \ln f_0}{\partial \ln q} = -i\frac{q}{\epsilon}(\hat{\mathbf{n}}\cdot\mathbf{k})k\delta\phi\frac{a^2 m^2}{q^2}\frac{\partial \ln m}{\partial \phi}\frac{\partial \ln f_0}{\partial \ln q}. \tag{31}$$

The Bolzmann hierarchy for neutrinos, obtained by expanding the perturbation Ψ in a Legendre series can be written as [24,25]

$$\dot{\Psi}_0 = -\frac{q}{\epsilon}k\Psi_1 + \frac{\dot{h}}{6}\frac{\partial \ln f_0}{\partial \ln q}, \tag{32}$$

$$\dot{\Psi}_1 = \frac{1}{3}\frac{q}{\epsilon}k\,(\Psi_0 - 2\Psi_2) + \kappa, \tag{33}$$

$$\dot{\Psi}_2 = \frac{1}{5}\frac{q}{\epsilon}k(2\Psi_1 - 3\Psi_3) - \left(\frac{1}{15}\dot{h} + \frac{2}{5}\dot{\eta}\right)\frac{\partial \ln f_0}{\partial \ln q}, \tag{34}$$

$$\dot{\Psi}_\ell = \frac{q}{\epsilon}k\left(\frac{\ell}{2\ell+1}\Psi_{\ell-1} - \frac{\ell+1}{2\ell+1}\Psi_{\ell+1}\right), \tag{35}$$

where

$$\kappa = -\frac{1}{3}\frac{q}{\epsilon}k\frac{a^2m^2}{q^2}\delta\phi\frac{\partial \ln m_\nu}{\partial\phi}\frac{\partial \ln f_0}{\partial \ln q}. \tag{36}$$

In our analysis, we consider three different types of quintessence potential: (1) inverse power law potentials (Model I), (2) SUGRA-type potential models (Model II), (3) exponential-type potentials (Model III), which are respectively, given by

$$V(\phi) = M^4\left(\frac{M_{\rm pl}}{\phi}\right)^\alpha; \quad M^4\left(\frac{M_{\rm pl}}{\phi}\right)^\alpha e^{3\phi^2/2M_{\rm pl}^2}; \quad M^4 e^{-\alpha(\phi/M_{\rm pl})}. \tag{37}$$

The coupling between cosmological neutrinos and dark energy quintessence could modify the CMB and matter power spectra significantly. It is therefore possible and also important to put constraints on coupling parameters from current observations. For this purpose, we use the WMAP3 [33,34] and 2dFGRS [35] datasets.

The flux power spectrum of the Lyman-α forest can be used to measure the matter power spectrum at small scales around $z < 3$ [36,37]. It has been shown, however, that the resultant constraint on neutrino mass can vary significantly from $\sum m_\nu < 0.2$ eV to 0.4 eV depending on the specific Lyman-α analysis used [38]. The complication arises because the result suffers from the systematic uncertainty regarding the model for the intergalactic physical effects, i.e., damping wings, ionizing radiation fluctuations, galactic winds, and so on [39]. Therefore, we conservatively omit the Lyman-α forest data from our current analysis.

Because there are many other cosmological parameters compared to Mass Varying Neutinos (MaVaNs) parameters, we follow the Markov chain Monte Carlo (MCMC) global fit approach [40] to explore the likelihood parameter space and marginalize over the nuisance parameters to obtain the constraint on parameters in which we are interested. Our parameter space consists of

$$\vec{P} \equiv (\Omega_b h^2, \Omega_c h^2, H, \tau, A_s, n_s, m_i, \alpha, \beta), \tag{38}$$

where $\omega_b h^2$ and $\Omega_c h^2$ are the baryon and CDM densities in units of critical density, H is the Hubble parameter, τ is the optical depth of Compton scattering to the last scattering surface, A_s and n_s are the amplitude and spectral index of primordial density fluctuations, and (m_i, α, β) are the parameters of MaVaNs.

As an example, the allowed space for the parameter are shown in figure 1 for Models I and III. In this figure, we do not observe the strong degeneracy between the introduced

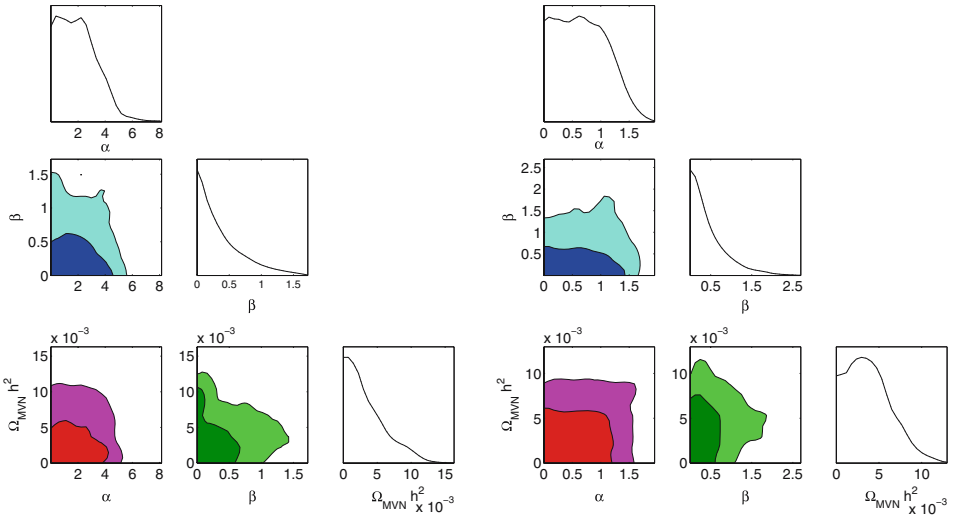

Figure 1. (**a**) Contours of constant relative probabilities in two-dimensional parameter planes for inverse power-law models. Lines correspond to 68% and 95.4% confidence limits. (**b**) Same as (**a**), but for exponential-type models.

parameters. That is why one can put tight constraints on MaVaNs parameters from the observations. Presently, for both models we consider that larger α leads to larger w. Therefore, large α is not allowed due to the same reason that larger w is not allowed from the current observations. We find no observational signature which favours the coupling between MaVaNs and quintessence scalar field, and obtain the upper limit on the coupling parameter as shown in table 3.

$$\beta < 0.46, 0.47, 0.58\ (1\,\sigma);\ \ [1.12, 1.36, 1.53\ (2\,\sigma)], \tag{39}$$

Table 3. Global analysis data within 2σ deviation for different types of quintessence potential.

Quantites	Model I	Model II	Model III	WMAP-3 data (ΛCDM)
α	< 4.38	0.10–11.82	< 1.41	–
β	< 1.12	< 1.36	< 1.53	–
$\Omega_B\,h^2[10^2]$	2.09–2.36	2.09–2.35	2.08–2.34	2.23 ± 0.07
$\Omega_{\rm CDM}\,h^2[10^2]$	9.87–12.30	9.85–12.40	9.84–12.33	12.8 ± 0.8
H_0	58.39–72.10	58.55–71.70	58.99–71.58	72 ± 8
Z_{re}	6.13–14.94	4.00–14.78	6.64–14.78	–
n_s	0.92–0.99	0.92–0.98	0.92–0.98	0.958 ± 0.016
$A_s[10^{10}]$	18.25–23.41	18.20–23.32	18.33–23.27	–
$\Omega_Q[10^2]$	57.43–75.60	57.59–75.02	58.45–75.05	71.6 ± 5.5
Age/Gyr	13.59–14.40	13.59–14.35	13.61–14.36	13.73 ± 0.16
$\Omega_{\rm MaVaNs}\,h^2[10^2]$	< 0.95	< 0.91	< 0.84	< 1.97 (95% CL)
τ	0.031–0.143	0.028–0.139	0.032–0.140	0.089 ± 0.030

Table 4. Global analysis data for the SUGRA-type quintessence potential (Model II) which is constrained by both WMAP3 and Ly-α forests.

Quantites	Mean	SDDEV	Lower 1σ	Upper 1σ	Lower 2σ	Upper 2σ	WMAP-3 data (ΛCDM)
α	6.65	2.98	5.01	7.92	2.24	12.26	–
β	0.42	0.42	0.00	0.47	0.00	1.35	–
$amnu_i$	0.02	0.02	0.00	0.02	0.00	0.07	–
$\Omega_B\, h^2[10^2]$	2.27	0.06	2.20	2.34	2.14	2.39	2.23 ± 0.07
$\Omega_{\rm CDM}\, h^2[10^2]$	12.22	0.56	11.65	12.78	11.19	13.39	12.8 ± 0.8
H_0	65.68	3.31	62.40	68.99	58.62	71.52	72 ± 8
Z_{re}	12.81	2.16	11.83	13.86	9.23	16.22	–
n_s	0.970	0.015	0.956	0.985	0.941	1.000	0.958 ± 0.016
$A_s[10^{10}]$	22.86	1.16	21.74	23.97	20.78	25.34	–
$\Omega_Q[10^2]$	66.11	4.47	61.75	70.48	56.18	73.42	71.6 ± 5.5
Age/Gyr	13.76	0.15	13.60	13.91	13.46	14.07	13.73 ± 0.16
$\Omega_{\rm MaVaNs}\, h^2[10^2]$	0.14	0.12	0.00	0.17	0.00	0.38	< 1.97 (95% CL)
τ	0.105	0.026	0.079	0.131	0.055	0.158	0.089 ± 0.030

and the present mass of neutrinos is also limited to

$$\Omega_\nu h^2_{\rm today} < 0.0044, 0.0048, 0.0048\ (1\,\sigma);\ \ [0.0095, 0.0090, 0.0084\ (2\,\sigma)], \tag{40}$$

for Models I, II and III, respectively (see table 4).

4. Results and discussions

Here we comment on some important points of this work: (1) Equation of states, (2) the impact of the scattering term of the Boltzmann equation, (3) the instability issue in our models and (4) neutrino mass bounds in the interacting neutrino dark-energy models.

(a) *Equation of states*: As pointed out by earlier works, it is possible to have the observational equation of state $w_{\rm eff}$ less than -1 in the neutrino-dark energy interacting models. The point is that any observer would be unaware of the dark energy interactions, and attribute any unusual evolution of neutrino energy density to dark energy. This is seen as follows. Let us consider the recent epoch where the neutrinos have already become massive enough so that the energy density of neutrinos can be described as

$$\rho_\nu = m_\nu(\phi) n_\nu = m_\nu(\phi) n_{\nu,0}/a^3, \tag{41}$$

where $n_\nu, 0$ is the number density of neutrinos at the present time. One can decompose this into two parts as

$$\rho_\nu = m_\nu(\phi_0) n_{\nu,0}/a^3 + \left(\frac{m_\nu(\phi)}{m_\nu(\phi_0)} - 1\right) m_\nu(\phi_0) n_{\nu,0}/a^3, \tag{42}$$

and hence the Friedmann equation (neglecting baryon and photon contributions)

$$H^2 = \frac{8\pi G}{3}\left(\rho_{\rm CDM} + \rho_\nu + \rho_\phi\right)$$
$$= \frac{8\pi G}{3}\left(\left(\rho_{\rm CDM,0} + \rho_{\nu,0}\right)/a^3 + \left(\frac{m_\nu(\phi)}{m_\nu(\phi_0)} - 1\right) m_\nu(\phi_0) n_{\nu,0}/a^3 + \rho_\phi\right). \quad (43)$$

Therefore, while the first term in the above equation is regarded as (total) matter density of our Universe, the second and third terms comprise effective energy density which would be recognized as dark energy,

$$\rho_{\rm eff} \equiv \left(\frac{m_\nu(\phi)}{m_\nu(\phi_0)} - 1\right) m_\nu(\phi_0) n_{\nu,0}/a^3 + \rho_\phi. \quad (44)$$

In observations, one measures the equation of state of dark energy $w_{\rm eff}$ defined by

$$\frac{{\rm d}\rho_{\rm eff}}{{\rm d}t} = -3H(1 + w_{\rm eff})\rho_{\rm eff}. \quad (45)$$

Here $w_{\rm eff}$ is related to the equation of state of quintessence w_ϕ through

$$w_{\rm eff} = \frac{w_\phi}{1 - x}, \quad (46)$$

$$x = \left(\frac{m_\nu(\phi)}{m_\nu(\phi_0)} - 1\right) \frac{m_\nu(\phi_0) n_{\nu,0}/a^3}{\rho_\phi}, \quad (47)$$

which are derived from eqs (21), (27) and (44). An example of time evolution of $w_{\rm eff}$ is depicted in figure 2.

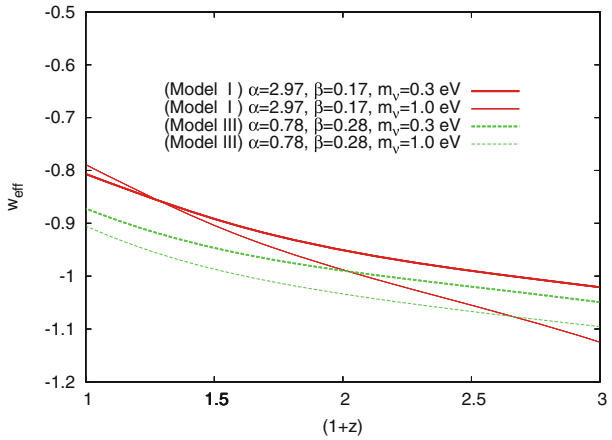

Figure 2. Time evolution of the effective equation of state parameter $w_{\rm eff}$ for models with potentials of inverse power law (Model I) and exponential types (Model III). The parameters are fixed to the best-fitting values except for those shown in the figure. The effective equation of state parameter can be smaller than -1 at $z > 0$.

(b) *Impact of the new scattering term*: Recently, perturbation equations for the MaVaNs models were nicely presented by Brookfield *et al* [30] (see also [31]) which are necessary to compute CMB and LSS spectra. The main difference here from their works is that we correctly take into account the scattering term in the geodesic equation of neutrinos, which was omitted there (see however, [41]). As the term is proportional to $\partial m/\partial x$ and first-order quantity in perturbation, our results and those of earlier works [30,31] remain the same in the background evolutions. However, neglecting this term violates the energy–momentum conservation law at linear level leading to the anomalously large ISW effect. As the term becomes important when neutrinos become massive, the late-time ISW is mainly affected by the interaction between dark energy and neutrinos. Consequently, the differences show up at large angular scales. In figure 3, the differences are shown with and without the scattering term. The early ISW can also be affected by this term to some extent in some massive neutrino models and the height of the first acoustic peak could be changed. However, the position of the peaks stays almost unchanged because the background expansion histories are the same.

(c) *Instability issue*: As shown in [42,43], some classes of models with mass-varying neutrinos suffer from the adiabatic instability at the first-order perturbation level. This is caused by an additional force on neutrinos mediated by the quintessence scalar field and occurs when its effective mass is much larger than the Hubble horizon scale, where the effective mass is defined by $m_{\rm eff}^2 = {\rm d}^2 V_{\rm eff}/{\rm d}\phi^2$. To remedy this situation one should consider an appropriate quintessential potential which has a mass comparable to the horizon scale at present, and the models considered in this paper are from [30]. Interestingly, some researchers have found that one can construct viable MaVaNs models by choosing certain couplings and/or quintessential potentials [44–46]. Some of these models even realize $m_{\rm eff} \gg H$. In figure 4, masses of the scalar field relative to the horizon scale $m_{\rm eff}/H$ are plotted. We find that $m_{\rm eff} < H$ for almost all periods and the models are stable. We also depict in

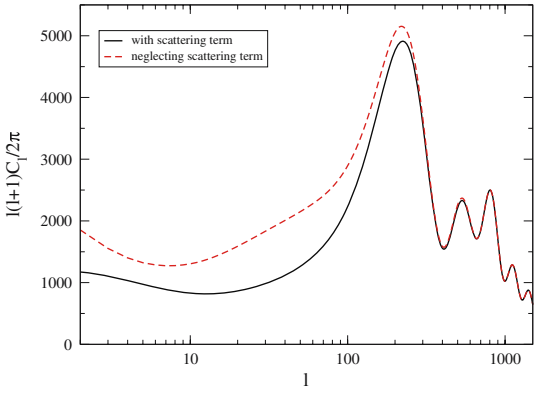

Figure 3. Differences between the CMB power spectra with and without the scattering term in the geodesic equation of neutrinos with the same cosmological parameters.

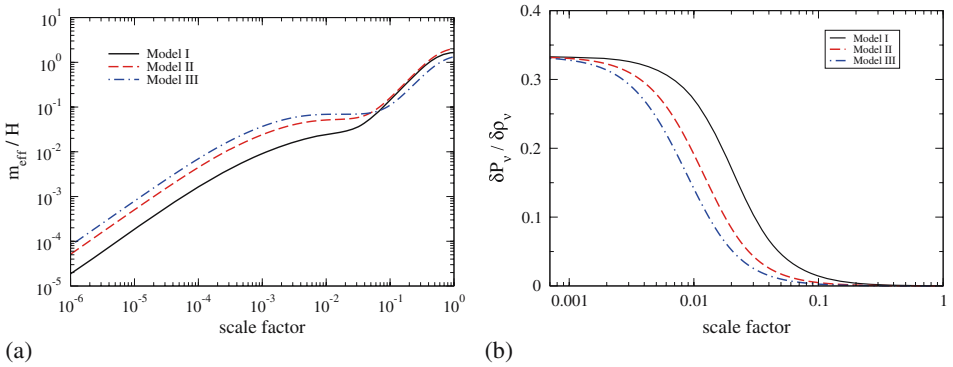

(a) (b)

Figure 4. (**a**) Typical evolution of the effective mass of the quintessence scalar field relative to the Hubble scale, for all models considered in this paper. (**b**) Typical evolution of the sound speed of neutrinos $c_s = \delta P_\nu/\delta\rho_\nu$ with the wavenumber $k = 2.3 \times 10^{-3}$ Mpc^{-1}, for models as indicated. The values stay positive starting from 1/3 (relativistic) and neutrinos are stable against the density fluctuation.

figure 4, the sound speed of neutrinos defined by $c_s^2 = \delta P_\nu/\delta\rho_\nu$ with the wavenumber $k = 2.3 \times 10^{-3}$ Mpc^{-1}.

(d) *Neutrino mass bounds*: When we apply the relation between the total sum of the neutrino masses M_ν and their contributions to the energy density of the Universe, $\Omega_\nu h^2 = M_\nu/(93.14\ \text{eV})$, we obtain the constraint on the total neutrino mass: $M_\nu < 0.87$ eV (95% CL) in the neutrino probe dark-energy model. The total neutrino mass contributions in the power spectrum is shown in figure 5, where we can see significant deviation from the observation data in the case of large neutrino masses.

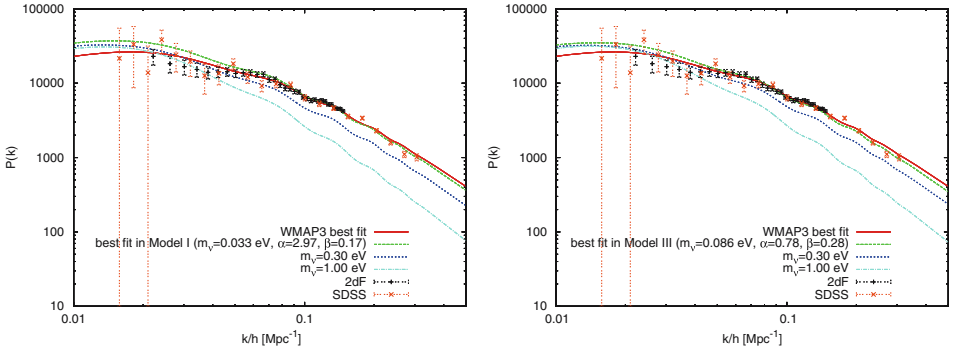

(a) (b)

Figure 5. Examples of the total mass contributions in the matter power spectrum in (**a**) Model I and (**b**) Model III. For both (**a**) and (**b**) we plot the best-fitting lines (green dashed), lines with larger neutrino masses $M_\nu = 0.3$ eV (blue dotted) and $M_\nu = 1.0$ eV (cyan dot–dashed) with the other parameters fixed to the best-fitting values. Note that while lines with $M_\nu = 0.3$ eV can fit to the data well by arranging the other cosmological parameters, lines with $M_\nu = 1.0$ eV cannot.

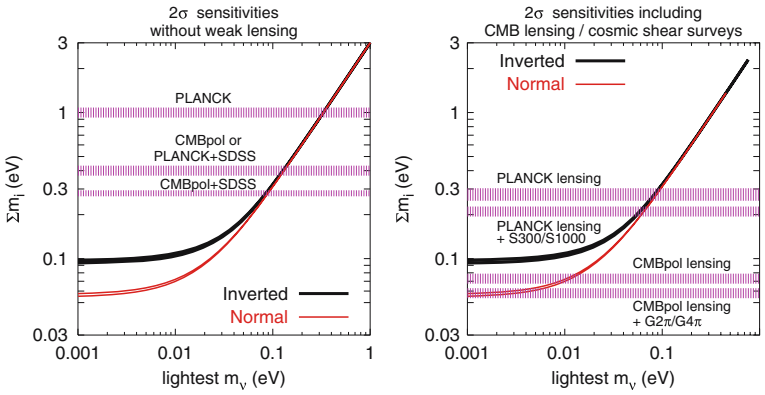

Figure 6. Forecast of 2σ sensitivities to the total neutrino mass from future cosmological experiments, compared to the values in agreement with the present neutrino oscillation data. (**a**) Sensitivities expected for future CMB experiments (without lensing extraction), alone and combined with the completed SDSS galaxy red-shift survey and (**b**) sensitivities expected for future CMB experiments including lensing information, alone and combined with future cosmic shear surveys. Here CMBpol refers to a hypothetical CMB experiment roughly corresponding to the inflation probe mission.

Beyond the scope of our current analysis, there are other possibilities in cosmological probes of neutrino masses:

(a) the evolution of cluster abundance with red-shit may provide further constraints on neutrino masses,
(b) the Lyman-α forest provides constraints on the matter power spectrum on a scale of $k \sim 1\,h\,\mathrm{Mpc}^{-1}$, where the effect of massive neutrinos is most viable,
(c) deep and wide weak lensing survey will make it possible, in the future, to perform weak lensing tomography of the matter density field.

As shown in figure 6, the combination of weak lensing tomography and high-precision CMB polarization experiments may reach sensitivities down to the lower bound of 0.06 eV on the sum of the neutrino masses [47–49]. In this case, normal hierarchy pattern will be detectable.

Acknowledgements

YYK is grateful to the organizers of UNICOS 2014 for the opportunity to present this work and for the warm hospitality. YYK would like to thank LAPTh at Annecy in France for the warm hospitality he has received during his visit there. His work is partially supported by the Research Professorship (A) of Ewha Womans University during 2010–2011, and by the Basic Science Research Programme through the National Research Foundation of Korea (NRF) funded by the Korean Ministry of Education, Science and Technology (Grant Nos 0409-20130121; 0409-20140077) and International Cooperation

Research Programme funded by the Korean Ministry of Science, ICT and Future Planning (Grant No. 0409-20130159).

References

[1] J Bonne *et al*, *Nuch. Phys. B (Proc. Suppl.)* **91**, 273 (2001)
[2] Ch Weinheimer, *Nucl. Phys. B (Proc. Suppl.)* **118**, 279 (2003)
[3] V A Rodin, A Faessler, F Simkovic and P Vogel, *Phys. Rev. C* **68**, 044302 (2003)
[4] Heidelberg-Moscow Collaboration: L Baudis *et al*, *Phys. Rev. Lett.* **83**, 41 (1999)
[5] IGEX Collaboration: C E Aalseth *et al*, *Phys. Rev. D* **65**, 092007 (2002); *Phys. Rev. D* **70**, 078302 (2004)
[6] G Mangano *et al*, *Nucl. Phys. B* **729**, 221 (2005)
[7] J F Beacom, N F Bell and S Dodelson, *Phys. Rev. Lett.* **93**, 121302 (2004)
[8] S Dodelson, A Melchiorri and A Slasar, *Phys. Rev. Lett.* **97**, 04031 (2006)
[9] S Hannestad, *J. Cosmol. Astropart. Phys.* **05**, 004 (2003)
[10] E Pierpaoli, *Mon. Not. R. Astron. Soc.* **342**, L63 (2003)
[11] S Hannestad, *J. Cosmol. Astropart. Phys.* **0502**, 011 (2005), arXiv:astro-ph/0411475
[12] A Slosar, *Phys. Rev. D* **73**, 123501 (2006)
[13] M Fukugita, K Ichikawa, M Kawasaki and O Lahav, *Phys. Rev. D* **74**, 027302 (2006)
[14] O Elgaroy *et al*, *Phys. Rev. Lett.* **89**, 061310 (2002)
O Elgaroy and O Lahav, *J. Cosmol. Astropart. Phys.* **0304**, 004 (2003)
[15] A G Sanchez *et al*, *Mon. Not. R. Astron. Soc.* **366**, 189 (2006)
[16] S Hannestad, *J. Cosmol. Astropart. Phys.* **0305**, 004 (2003)
[17] V Barger, D Marfatia and A Tregre, *Phys. Lett. B* **595**, 55 (2004)
[18] WMAP Collaboration: D N Spergel *et al*, astro-ph/0603449
[19] A Goodbar, S Hannestad, E Mortsell and H Tu, *J. Cosmol. Astropart. Phys.* **06**, 019 (2006)
[20] U Seljak, A Slosar and P McDonald, *J. Cosmol Astropart. Phys.* **10**, 014 (2006)
[21] W Hu, D J Eisenstein and M Tegmark, *Phys. Rev. Lett.* **80**, 5255 (1998), arXiv: astro-ph/9712057
[22] J R Bond, G Efstathiou and J Silk, *Phys. Rev. Lett.* **45**, 1980 (1980)
[23] K Ichikawa, M Fukugita and M Kawasaki, *Phys. Rev. D* **71**, 043001 (2005)
[24] K Ichiki and Y-Y Keum, *J. Cosmol. Astropart. Phys.* **0806**, 005 (2008)
[25] Y-Y Keum, *Mod. Phys. Lett.* **A22**, 2131 (2007)
[26] K Ichiki and Y-Y Keum, *J. High Energy Phys.* **0806**, 058 (2008)
[27] D B Kaplan, A E Nelson and N Weiner, *Phys. Rev. Lett.* **93**, 091801 (2004)
R D Peccei, *Phys. Rev. D* **71**, 023527 (2005)
[28] R Fardon, A E Nelson and N Weiner, *J. Cosmol. Astropart. Phys.* **0410**, 005 (2004), arXiv:astro-ph/0309800
[29] X J Bi, P h Gu, X l Wang and X M Zhang, *Phys. Rev. D* **69**, 113007 (2004), arXiv:hep-ph/0311022
[30] A W Brookfield, C van de Bruck, D F Mota, and D Tocchini-Valentini, *Phys. Rev. Lett.* **96**, 061301 (2006); *Phys. Rev. D* **73**, 083515 (2006)
[31] G B Zhao, J Q Xia and X M Zhang, arXiv:astro-ph/0611227
[32] C P Ma and E Bertschinger, *Astrophys. J.* **455**, 7 (1995)
[33] WMAP Collaboration: G Hinshaw *et al*, arXiv:astro-ph/0603451
[34] WMAP Collaboration: L Page *et al*, arXiv:astro-ph/0603450
[35] The 2dFGRS Collaboration: S Cole *et al*, *Mon. Not. R. Astron. Soc.* **362**, 505 (2005), arXiv:astro-ph/0501174
[36] P McDonald, J Miralda-Escude, M Rauch, W L W Sargent, T A Barlow, R Cen and J P Ostriker, *Astrophys. J.* **543**, 1 (2000), arXiv:astro-ph/9911196

[37] R A C Croft *et al*, *Astrophys. J.* **581**, 20 (2002), arXiv:astro-ph/0012324
[38] A Goobar, S Hannestad, E Mortsell and H Tu, *J. Cosmol. Astropart. Phys.* **0606**, 019 (2006), arXiv:astro-ph/0602155
[39] P McDonald, U Seljak, R Cen, P Bode and J P Ostriker, *Mon. Not. R. Astron. Soc.* **360**, 1471 (2005), arXiv:astro-ph/0407378
[40] A Lewis and S Bridle, *Phys. Rev. D* **66**, 103511 (2002)
[41] A W Brookfield, C van de Bruck, D F Mota and D Tocchini-Valentini, *Phys. Rev. D* **76**, 049901 (2007)
[42] N Afshordi, M Zaldarriaga and K Kohri, *Phys. Rev. D* **72**, 065024 (2005)
[43] R Bean, E E Flanagan and M Trodden, arXiv:0709.1128 [astro-ph]
[44] M Kaplinghat and A Rajaraman, *Phys. Rev. D* **75**, 103504 (2007)
[45] O E Bjaelde, A W Brookfield, C van de Bruck, S Hannestad, D F Mota, L Schrempp and D Tocchini-Valentini, arXiv:0705.2018 [astro-ph]
[46] R Takahashi and M Tanimoto, *J. High Energy Phys.* **0605**, 021 (2006)
[47] Y S Song and L Knox, *Phys. Rev. D* **70**, 063510 (2004)
[48] S Hannestad, H Tu and Y Y Y Wong, *J. Cosmol. Astropart. Phys.* **0606**, 025 (2006)
[49] J Lesgourgues and S Pastor, *Phys. Rep.* **429**, 307 (2006)